

Supporting Information

Eco-Safe Degradation of Reactive Orange 16 via Adsorption-Enhanced Photocatalysis Using CoFe₂O₄ Nanoparticles

Nasira Hussain¹, Muhammad Bilal^{2*}, Younas Afzal¹, Shanza Shafaat¹, Bilal Ahmad Zafar Amin³
Faheem Shah^{4*}, Ahson Jabbar Shaikh^{1*}

¹Department of Chemistry, COMSATS University Islamabad, Abbottabad Campus, Abbottabad – 22060, KPK, Pakistan

²Department of Environmental Sciences, COMSATS University Islamabad, Abbottabad Campus, Abbottabad – 22060, KPK, Pakistan

³Department of Chemical Engineering, COMSATS University Islamabad - Lahore Campus, Lahore, Punjab, Pakistan.

⁴Department of Chemistry, College of Science, King Faisal University, Hofuf, Eastern Province ALAhsa – 31982, Kingdom of Saudi Arabia

***Corresponding authors:**

mbilal@cuiatd.edu.pk (Prof. Dr. Muhammad Bilal)

fshah@kfu.edu.sa (Dr. Faheem Shah)

ahson@cuiatd.edu.pk (Dr. Ahson Jabbar Shaikh)

Study of the Adsorption Isotherms

Adsorption isotherm models serve as mathematical tools extensively employed to characterize various aspects, such as molecule coverage, surface homogeneity/heterogeneity of NPs, binding energies, the physical/chemical nature of interactions, and the adsorption heat associated with molecules.

Freundlich Model

The Freundlich adsorption isotherm gives an expression (equation 1) encompassing the surface heterogeneity and the exponential distribution of active sites and their energies. The compounds which have the greater K_f values have high affinity toward the adsorbent as compared to others having low K_f value; the relatively high correlation coefficients indicate that the experimental data agree well with the Freundlich adsorption isotherm model [1, 2]. The value of $1/n$ determines the isotherm type in which $1/n = 0$, $0 < 1/n < 1$ and $1/n > 1$ indicate irreversible, favorable, and unfavorable isotherms respectively.

$$\ln q_e = \ln K_f + \frac{1}{n} \ln C_e \quad (1)$$

K_f and $1/n$ can be determined from intercept and slope of plot $\log(q_e)$ versus $\log(C_e)$ respectively.

Langmuir Model

The Langmuir isotherm assumes a monolayer adsorption of adsorbate molecules onto the surface of adsorbent mainly via chemical interaction [3].

$$\frac{1}{q_e} = \left(\frac{1}{K_L q_{max}} \right) \frac{1}{C_e} + \frac{1}{q_{max}} \quad (2)$$

In this equation 2, C_e represents the concentration at equilibrium (mg./g), q_{max} denotes the maximum adsorption capacity of adsorbent (mg/g) and K_L stands for Langmuir constant which is used to determine the maximum energy of adsorption related to the area occupied by adsorbent. R_L is a dimensionless constant separation factor [4-6].

Temkin Isotherm Model

This model (equation 3) used when adsorption heat decreases linearly with coverage because of the adsorbent-adsorbate interactions [7].

$$q_e = \frac{RT}{B_T} \ln(A_T C_e) \quad (3)$$

where q_e is the amount of dye adsorbed at equilibrium (mg/g), C_e is the equilibrium dye concentration in solution (mg/L), R is the universal gas constant (8.314 J/mol·K), T is the absolute temperature (K), B_T is a constant related to the heat of adsorption (J/mol), and A_T is the equilibrium binding constant (L/g).

Redlich–Peterson Isotherm Model

Redlich–Peterson isotherm equates (equation 4) the Langmuir and Freundlich systems and includes the advantages of both models instead of conflicts between the two system [8].

$$\log \frac{q_e}{C_e} = \ln(K_R) - g \log(C_e) \quad (4)$$

Error Function Test

Various error functions were investigated to find the best and most appropriate model for investigating equilibrium data. The hybrid error function (equation 5) overcomes the limitations of conventional error metrics at low concentrations by improving fitting sensitivity. It penalizes deviations relative to measured values rather than using absolute errors alone [9].

$$\text{Hybrid} = \frac{100}{N-P} \sum \frac{q_{e_{exp}} - q_{e_{cal}}}{q_{e_{exp}}} \quad (5)$$

where N is the total number of data points, $q_{e_{exp}}$ and $q_{e_{cal}}$ (mg/g) are the experimental and calculated adsorption capacities, and P is the number of isotherm parameters. The nonlinear chi-square test evaluates the goodness of fit by quantifying the weighted squared deviations between experimental and predicted values, as expressed in equation 6 [10].

$$X^2 = \frac{(q_{e_{exp}} - q_{e_{cal}})^2}{q_{e_{exp}}} \quad (6)$$

The sum of absolute errors (EABS) measures how closely the model matches the experimental data by calculating the absolute difference between them, though it may favor high-concentration data as errors increase with larger values. While average percentage error (APE) represents the mean relative deviation between experimental and predicted data. Equation 7 and 8 used to calculate EABS and APE errors [11].

$$EABS = \sum_{i=1}^N (q_{e_{exp}} - q_{e_{cal}}) \quad (7)$$

$$APE = \frac{100}{N} \sum_{i=1}^N \frac{q_{e_{exp}} - q_{e_{cal}}}{q_{e_{exp}}} \quad (8)$$

Kinetic Modeling

Kinetic adsorption studies are essential in the optimization of conditions governing the adsorption process for pollutant adsorption. The kinetic data was analyzed using several kinetic models including pseudo-first-order pseudo-second order and intraparticle diffusion model models.

Pseudo 1st order Kinetics

The pseudo-first order (PFO) model, originally proposed by Lagergren (1898), is one of the most widely applied kinetic models to describe adsorption processes. It assumes that the rate of change

of solute uptake with time is directly proportional to the difference between the equilibrium adsorption capacity and the amount adsorbed at any given time [12]. The linear formula of the pseudo-first-order kinetics is expressed in equation 9.

$$\log (q_e - q_t) = \log q_e - \frac{k_1}{2.303} t \quad (9)$$

Here, q_e represents the equilibrium amount of the adsorbate absorbed in mg/g of the adsorbent, q_t denotes the quantity adsorbed in mg/g of the adsorbate at time t , and k_1 (min^{-1}) stands for the pseudo-first-order rate constant.

Pseudo-Second-Order Kinetics

The pseudo-second order (PSO) kinetic model, developed by Ho and McKay, is widely used to describe adsorption processes where chemisorption is the rate-controlling step. The model assumes that the adsorption rate is proportional to the square of the number of unoccupied sites [13]. The pseudo-second-order equation (10) is as follows:

$$\frac{t}{q_t} = \frac{1}{K_2 q_e^2} + \frac{t}{q_t} \quad (10)$$

where K_2 denotes the second-order rate constant (g/mg/min). Plotting (t/q_t) versus (t) yields a linear relationship, and the slope and intercept can be used to derive the q_e and K_2 parameters, respectively.

Intraparticle Diffusion Model

The intraparticle diffusion model proposed by Weber and Morris is widely employed to investigate the rate-controlling steps in adsorption processes. It helps determine whether diffusion of adsorbate molecules into the pores of the adsorbent is the limiting mechanism. The model is expressed in equation 11.

$$q_t = k_p t^{1/2} + C \quad (11)$$

where k_p is the intraparticle diffusion rate constant ($\text{min}^{-1/2}$) which can be determined from the plot of q_t vs $t^{1/2}$ and C is intercept.

Thermodynamic of Adsorption

The thermodynamic parameters including change in enthalpy (ΔH) and entropy (ΔS) were computed using Van't Hoff equation (equation 12).

$$\ln K_d = \frac{\Delta S}{R} - \frac{\Delta H}{RT} \quad (12)$$

The distribution coefficient K_d was calculated from equation 13.

$$K_d = \frac{q_e}{C_e} \quad (13)$$

Here q_e (mg/g) is the solid phase concentration and C_e (mg/L) is the liquid phase concentration at equilibrium. Change in Gibbs free energy (ΔG) was determined using equation 14.

$$\Delta G = \Delta H - T\Delta S \quad (14)$$

Equilibrium Adsorption Isotherms Models

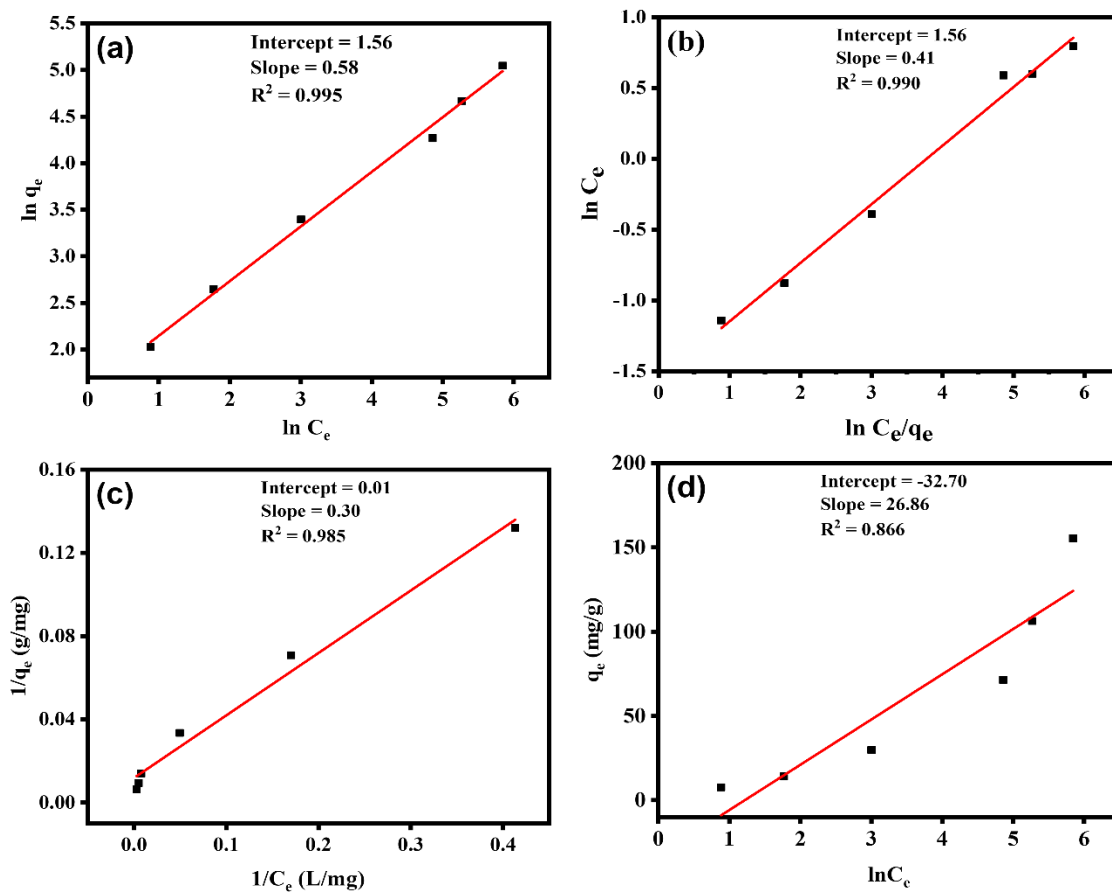


Figure S1. Adsorption study of RO16 dye on CoFe₂O₄ NPs: equilibrium adsorption data fitted to isotherm models (a) Freundlich, (b) Redlich–Peterson, (c) Langmuir, and (d) Temkin

Equilibrium Kinetics and Thermodynamic Analysis

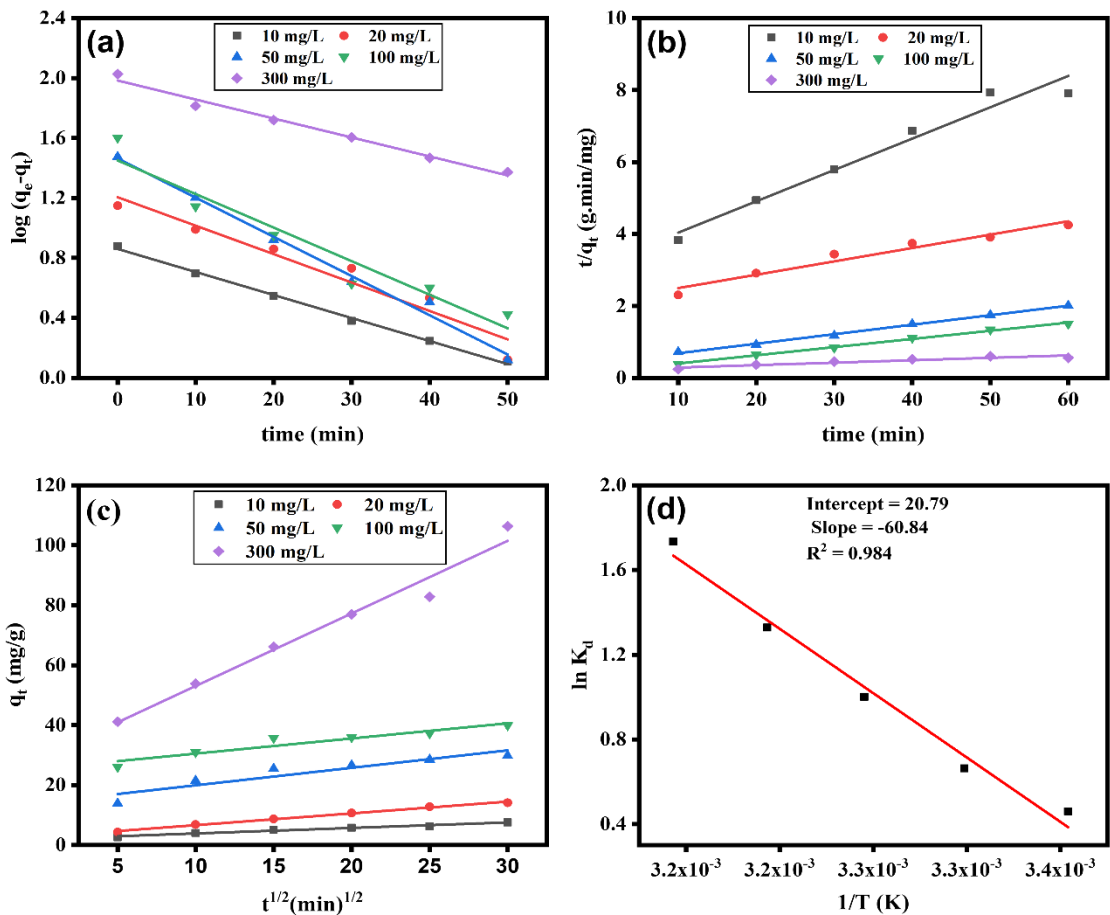


Figure S2. Adsorption study of RO16 dye on CoFe₂O₄ NPs. (a–c) kinetic models (PFO, PSO, IPD); (d) Van't Hoff plot. Experimental conditions: dose = 1 mg/g, solution pH, T = 298.15 K, C₀ = 20 mg/L.

Tomato Seed Germination and Antibacterial Study of CoFe₂O₄ NPs

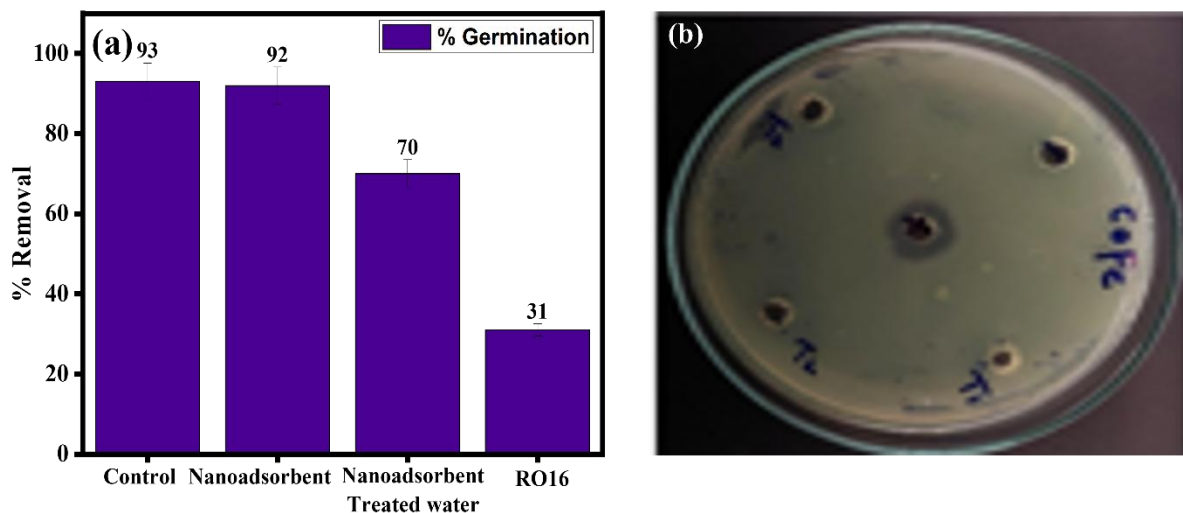


Figure S3. CoFe₂O₄NPs (a) Tomato seed germination toxicity assay (b) A cell cytotoxicity test against *Pseudomonas aeruginosa* PAO1. Various treatments (T1, T2, T3) are compared with the positive control (+).

Desorption efficiency of CoFe₂O₄ NPs

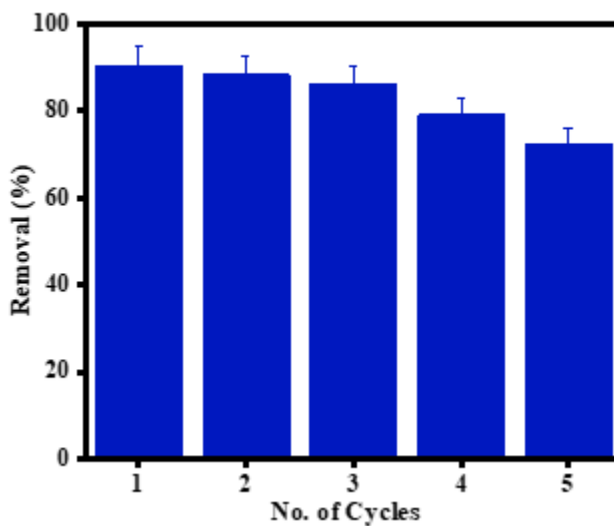


Figure S4. Desorption efficiency of RO16 from CoFe₂O₄ NPs.

References

1. Othman, C.S., Y.M. Salih, and L.O. Hamasalih, *Adsorption desulfurization of dibenzothiophene in a model and diesel fuel by hybrid activated charcoal/mixed metal oxide*. Petroleum Science and Technology, 2023. **41**(22): 2121-2140.
2. Ajibade, P.A. and E.C. Nnadozie, *Synthesis, characterization, and structural studies of biochar capped magnetic iron oxide and its potentials as adsorbents for organic dyes*. Case Studies in Chemical and Environmental Engineering, 2023. **8**: 100473.
3. Birniwa, A.H., et al., *Adsorption behavior of methylene blue cationic dye in aqueous solution using polypyrrole-polyethylenimine nano-adsorbent*. Polymers, 2022. **14**(16): 3362.
4. Kumar, K.Y., et al., *Low-cost synthesis of metal oxide nanoparticles and their application in adsorption of commercial dye and heavy metal ion in aqueous solution*. Powder technology, 2013. **246**: 125-136.
5. McKay, G., et al., *Adsorption of reactive dye from aqueous solutions by compost*. Desalination and water treatment, 2011. **28**(1-3): 164-173.
6. Ashour, M., et al., *Equilibrium and Kinetic Modeling of Crystal Violet Dye Adsorption by a Marine Diatom, Skeletonema costatum*. Materials, 2022. **15**(18): 6375.
7. Mudhoo, A., *Unveiling new Insights: Revised Temkin adsorption isotherm parameters from fresh Curve fits in adsorption studies*. Chemical Engineering Science, 2025. **311**: 121585.
8. Ganthavee, V. and A. Trzcinski, *Removal of reactive black 5 in water using adsorption and electrochemical oxidation technology: kinetics, isotherms and mechanisms*. International Journal of Environmental Science and Technology, 2025. **22**(2): 1083-1106.
9. Ayawei, N., A.N. Ebelegi, and D. Wankasi, *Modelling and interpretation of adsorption isotherms*. Journal of chemistry, 2017. **2017**(1): 3039817.
10. Okpara, O.G., et al., *Optimum isotherm by linear and nonlinear regression methods for lead (II) ions adsorption from aqueous solutions using synthesized coconut shell-activated carbon (SCSAC)*. Toxin Reviews, 2021. **40**(4): 901-914.
11. Mansour, A.T., et al., *Dried brown seaweed's phytoremediation potential for methylene blue dye removal from aquatic environments*. Polymers, 2022. **14**(7): 1375.
12. Tran, H.N., *Differences between chemical reaction kinetics and adsorption kinetics: Fundamentals and discussion*. Journal of Technical Education Science, 2022. **17**(Special Issue 01): 33-47.
13. Tran, H.N., *Is it possible to draw conclusions (adsorption is chemisorption) based on fitting between kinetic models (pseudo-second-order or elovich) and experimental data of time-dependent adsorption in solid-liquid phases?* 2022, Bentham Science Publishers direct. 228-230.